

# On the calculation of the bandgap of periodic solids with MGGA functionals using the total energy

Fabien Tran,<sup>1</sup> Jan Doumont,<sup>1</sup> Peter Blaha,<sup>1</sup> Miguel A. L. Marques,<sup>2</sup> Silvana Botti,<sup>3</sup> and Albert P. Bartók<sup>4,5</sup>

<sup>1</sup>*Institute of Materials Chemistry, Vienna University of Technology, Getreidemarkt 9/165-TC, A-1060 Vienna, Austria*

<sup>2</sup>*Institut für Physik, Martin-Luther-Universität Halle-Wittenberg, D-06099 Halle, Germany*

<sup>3</sup>*Institut für Festkörperteorie und -optik, Friedrich-Schiller-Universität Jena and European Theoretical Spectroscopy Facility, Max-Wien-Platz 1, 07743 Jena, Germany*

<sup>4</sup>*Rutherford Appleton Laboratory, Scientific Computing Department Science and Technology Facilities Council, Didcot OX11 0QX, United Kingdom*

<sup>5</sup>*Department of Physics and Warwick Centre for Predictive Modelling, School of Engineering, University of Warwick, Coventry, CV4 7AL, United Kingdom*

(Dated: 4 November 2019)

During the last few years, it has become more and more clear that functionals of the meta generalized gradient approximation (MGGA) are more accurate than GGA functionals for the geometry and energetics of electronic systems. However, MGGA functionals are also potentially more interesting for the electronic structure, in particular when the potential is non-multiplicative (i.e., when MGGA are implemented in the generalized Kohn-Sham framework), which may help to get more accurate bandgaps. Here, we show that the calculation of bandgap of solids with MGGA functionals can be done very accurately also in a non-self-consistent manner. This scheme uses only the total energy and can, therefore, be very useful when the self-consistent implementation of a particular MGGA functional is not available. Since self-consistent MGGA calculations may be difficult to converge, the non-self-consistent scheme may also help to speed-up the calculations. Furthermore, it can be applied to any other types of functionals, for which the implementation of the corresponding potential is not trivial.

In density functional theory (DFT)<sup>1</sup> implemented using an auxiliary system of noninteracting electrons, either within the Kohn-Sham (KS)<sup>2</sup> or generalized KS (gKS)<sup>3</sup> framework, the difference between the energies of the highest occupied (HO) and lowest unoccupied (LU) orbitals,

$$E_g^{(g)KS} = \epsilon_{LU} - \epsilon_{HO}, \quad (1)$$

is often used to calculate the fundamental (photoemission) bandgap  $E_g$ . It is defined formally as ( $N$  is the number of electrons in the system)

$$E_g = I(N) - A(N) \\ = [E_{\text{tot}}(N-1) - E_{\text{tot}}(N)] - [E_{\text{tot}}(N) - E_{\text{tot}}(N+1)], \quad (2)$$

where  $I$  and  $A$  are the ionization potential and electron affinity, respectively. However, within the KS framework,<sup>2</sup> i.e., with a multiplicative exchange-correlation potential  $v_{xc} = \delta E_{xc} / \delta \rho$ ,  $E_g^{KS}$  and  $E_g$  differ:

$$E_g = I(N) - A(N) = -\epsilon_{HO}(N) - [-\epsilon_{HO}(N+1)] \\ = \underbrace{\epsilon_{LU}(N) - \epsilon_{HO}(N)}_{E_g^{KS}} + \underbrace{\epsilon_{HO}(N+1) - \epsilon_{LU}(N)}_{\Delta_{xc}} \\ = E_g^{KS} + \Delta_{xc}, \quad (3)$$

where  $\Delta_{xc}$  is the derivative discontinuity.<sup>4,5</sup> As a consequence, with most functionals, either the (unknown) exact one or a standard approximation of the local density approximation (LDA) or generalized gradient approximation (GGA),<sup>6-8</sup>  $\epsilon_{LU} - \epsilon_{HO}$  is (much) smaller than the value of  $E_g$  obtained from experiment<sup>9</sup> (note that very often the experimental bandgap is obtained from optical experiment, which however is direct and includes the excitonic effect). Nevertheless, a few

points should be mentioned. First, for a periodic solid it was proven that  $\Delta_{xc} = 0$  with LDA/GGA<sup>10,11</sup> (but  $\epsilon_{LU} - \epsilon_{HO}$  is still smaller than  $E_g$ ). Second, the self-interaction error (SIE)<sup>12</sup> (or delocalization error<sup>13</sup>) may also worsen the discrepancy between  $E_g$  and  $E_g^{KS}$ , and actually the absence of a derivative discontinuity and the SIE are difficult to disentangle.<sup>14</sup> Third, within KS-DFT there exist specialized functionals that are able to provide values of  $\epsilon_{LU} - \epsilon_{HO}$  close to  $E_g$ .<sup>15-17</sup>

Within the gKS theory,<sup>3</sup> which concerns functionals  $E_{xc}$  that are not explicit functionals of the electron density  $\rho$ ,  $\Delta_{xc}$  (or a part of it) is included in  $E_g^{gKS} = \epsilon_{LU} - \epsilon_{HO}$  [i.e., Eq. (3) does not hold in gKS theory]. Meta-GGA (MGGA)<sup>18</sup> and hybrid functionals<sup>19</sup> are usually implemented with a gKS Hamiltonian and should in principle be able to provide bandgaps that are more accurate than with GGA. This also means that a direct comparison of  $E_g^{gKS}$  and  $E_g$  is more justified than in the KS theory.<sup>20-23</sup>

MGGA methods are very attractive since they are of the semilocal type, therefore computationally efficient, and they have shown to be overall more accurate than GGA functionals for the geometry and energetics of molecules and solids. This is for instance the case with the recent SCAN functional,<sup>24</sup> which has attracted a lot of attention, see e.g., Refs. 25 and 26 (in passing we note that SCAN reduces the SIE,<sup>27,28</sup> but on the other hand leads to over-localization and therefore too large magnetic moments in itinerant metals<sup>25,29-31</sup>). Thus, MGGA functionals are very interesting and promising.

The focus of the present work is on the calculation of the bandgap of solids with MGGA functionals. We will show that the bandgap can be calculated very accurately non-self-consistently using the total energy with Eq. (2). This procedure is very useful when a self-consistent implementa-

tion of MGGAs<sup>32</sup> is not available or the computational effort needs to be reduced (MGGAs can be notably more expensive than GGAs<sup>33,34</sup> and may require more iterations to achieve self-consistent field convergence). Thus, the proposed scheme may also be very helpful to apply MGGAs more efficiently in applications involving very large systems or for high-throughput materials screening.

Contrary to the common belief<sup>35,36</sup> that using Eq. (2) for the calculation of the bandgap of periodic systems is technically difficult and poses problems, it has been recently underlined in Refs. 11, 23, and 37 (see also a related discussion in Ref. 38) that it is not the case. Here, Eq. (2) is used to calculate  $E_g$  with MGGAs functionals. Briefly,  $E_{\text{tot}}(N-1)$ , the total energy of the whole solid which consists of  $N_k$  unit cells (i.e., the number of  $\mathbf{k}$  points in the first Brillouin zone used in the calculation) and  $N$  electrons is evaluated with the electron density  $\rho^{N-1} = \rho^N - (1/N_k)|\psi_{\text{HO}}|^2$  and kinetic-energy density  $t^{N-1} = t^N - (1/N_k)(1/2)\nabla\psi_{\text{HO}}^* \cdot \nabla\psi_{\text{HO}}$ , where  $\psi_{\text{HO}}$  is the orbital at the valence band maximum and is normalized to one in the unit cell. Similarly, the contribution from the orbital  $\psi_{\text{LU}}$  at the conduction band minimum is added to  $\rho^N$  and  $t^N$  to calculate  $E_{\text{tot}}(N+1)$ . Since in the limit of an infinite solid ( $N_k \rightarrow \infty$ ) the addition or subtraction of a single electron has no effect on the orbitals, the three total energies in Eq. (2) can be evaluated with the orbitals obtained from the calculation of the neutral  $N$ -electron system. Usually, DFT codes with periodic boundary conditions deliver the total energy per unit cell (uc)  $E_{\text{tot}}^{\text{uc}}$ , therefore in Eq. (2)  $E_{\text{tot}} = N_k E_{\text{tot}}^{\text{uc}}$ . We mention that adding or not adding a background charge to make the  $N-1$ - and  $N+1$ -electron systems neutral leads to the same results for  $E_g$  when the calculation is converged with  $N_k$ . As in Ref. 23, we checked that Eqs. (1) and (2) lead to exactly the same bandgap for a GGA.

With the goal of applying Eq. (2) to a MGGAs non-self-consistently without having access to the orbitals (and density) generated with the corresponding non-multiplicative MGGAs potential, the central technical question is which set of orbitals should be used. Our procedure is the following. For a given MGGAs functional  $E_{\text{xc}}$ , the total energy is evaluated with various sets of GGA orbitals. The best set is the one leading to the lowest (i.e., most negative) total energy, since according to the variational principle, the lower the total energy, the closer one should approach the true MGGAs orbitals of a self-consistent calculation. Note that a similar procedure has been used for self-interaction corrected functionals.<sup>39</sup>

In order to test the accuracy of the procedure, the MGGAs energy functionals  $E_{\text{xc}}$  that we chose to calculate the bandgap are TPSS,<sup>40</sup> revTPSS,<sup>41</sup> MVS,<sup>42</sup> SCAN,<sup>24</sup> rSCAN,<sup>43</sup> TM,<sup>44</sup> and HLE17.<sup>45</sup> The existing GGA potentials  $v_{\text{xc}}$  that were used to generate the orbitals are PBE,<sup>6</sup> RPBE,<sup>46</sup> PBEsol,<sup>47</sup> EV93PW91,<sup>48,49</sup> AK13,<sup>16</sup> HCTH407,<sup>50</sup> and HLE16.<sup>17</sup> An additional GGA potential that we also considered consists of a modified RPBE potential (mRPBE), where the exchange and correlation components are multiplied by 1.25 and 0.5, respectively. The construction of mRPBE is motivated by the fact that the MGGAs HLE17 is a modification of TPSS, with exchange and correlation multiplied by also 1.25 and 0.5, and, as shown below, the RPBE potential is the preferred

one for generating orbitals to use with TPSS. Besides these eight GGA potentials, the LDA,<sup>2,51</sup> LB94,<sup>52</sup> and Slocc<sup>53</sup> potentials were also considered for generating the orbitals. The hope is that among these multiplicative potentials, there is one providing orbitals that are reasonably close to the ones that would be obtained with the non-multiplicative MGGAs potential. If this is the case, then the bandgap calculated using Eq. (2) with the GGA orbitals should be close to the bandgap  $E_g^{\text{gKS}} = \epsilon_{\text{LU}} - \epsilon_{\text{HO}}$  calculated self-consistently with the MGGAs potential. Ideally, and in order to have a scheme that is useful in practice, it should be always (or at least for most solids) the same set of GGA orbitals (for a given MGGAs) that leads to the most negative MGGAs total energy and, hopefully, to a bandgap that is close to the true self-consistent one.

The WIEN2k code,<sup>54</sup> a full-potential and all-electron code based on the linearized augmented plane-wave method,<sup>55,56</sup> has been used for the calculations. For each of the 30 solids that we considered (*sp*-semiconductors, wide bandgap ionic insulators, and rare gases, see Table I), the MGGAs total energy was evaluated with the 11 different sets of GGA orbitals. We found that for most solids this is the same set that leads to the most negative MGGAs total energy. However, as expected, the set of *optimal* orbitals depends on the MGGAs functional under consideration. Those are the ones that were generated from EV93PW91 for MVS, mRPBE for HLE17, and RPBE for the other MGGAs.

Using these *optimal* orbitals, the results for the bandgap are shown in Table I. The calculations were done at the experimental geometry.<sup>57</sup> Comparison is made with the bandgaps obtained using the VASP code<sup>58</sup> (based on the projector augmented wave method<sup>59</sup>), which allows for self-consistent MGGAs calculations (details of the calculations can be found in Ref. 57). Additional self-consistent pseudopotential calculations for the PBE and rSCAN functionals (with pseudopotentials generated specifically for the respective functional) were performed with the CASTEP code.<sup>60,61</sup> It is shown that the agreement between WIEN2k and VASP is often very good, since the difference is below 0.1 eV in the majority of cases except for MVS (using the EV93PW91 orbitals). The largest discrepancies, 0.54 eV for Ge and 0.43 eV for Ne, were obtained with MVS. In the case of Ne, a discrepancy of this order of magnitude is acceptable since it is rather small compared to the bandgap which is above 13 eV. However, this is not the case for Ge, since 0.54 eV represents 45% of the MVS bandgap of 1.22 eV calculated with VASP. Other differences between WIEN2k and VASP which are relatively important are obtained for AIAs and AISb with HLE17, and for ZnO with SCAN and rSCAN. Actually, for the latter functional the CASTEP bandgaps agree in general extremely well with those from VASP (in the same way as with PBE), which indicates that the WIEN2k/VASP discrepancies should be due to the non-self-consistent procedure. MVS and HLE17 lead to bandgaps that are clearly larger than with all other functionals, therefore these two functionals are somehow different. This means that for these two functionals, some (occasional) non-negligible error due to the use of an inconsistent pseudopotential should not be completely excluded.

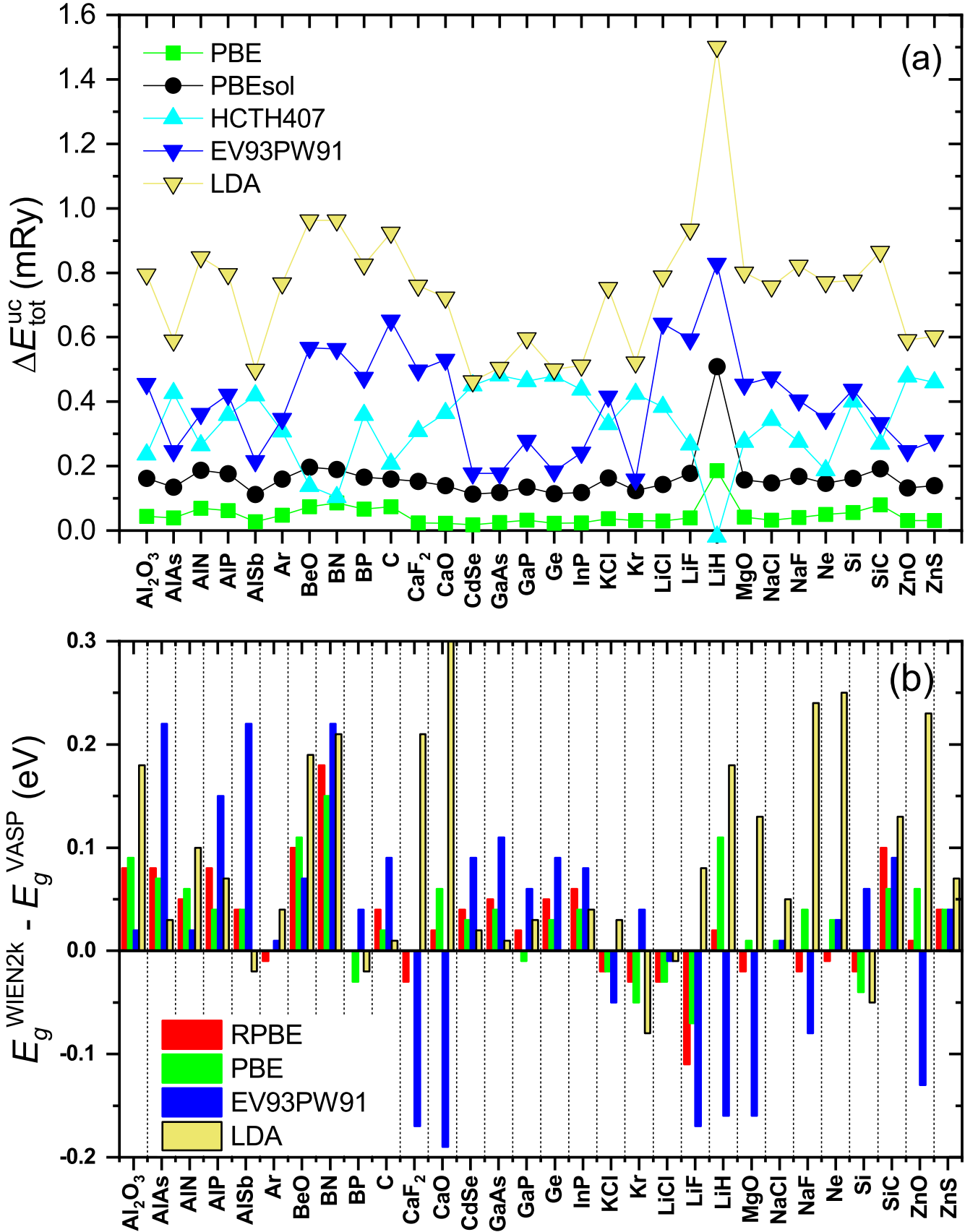


FIG. 1. Results obtained with the revTPSS functional using different sets of orbitals. (a) Total energy with respect to the value obtained with the RPBE orbitals,  $\Delta E_{\text{tot}}^{\text{uc}} = (E_{\text{tot}}^{\text{uc}}[\{\psi_i\}] - E_{\text{tot}}^{\text{uc}}[\{\psi_i^{\text{RPBE}}\}]) / N_{\text{el}}^{\text{uc}}$ , where  $E_{\text{tot}}^{\text{uc}}$  is in mRy and  $N_{\text{el}}^{\text{uc}}$  is the number of electrons per unit cell. (b) Bandgap difference  $E_g^{\text{WIEN2k}} - E_g^{\text{VASP}}$ . For clarity, the results with PBEsol and HCTH407 are not shown.

TABLE I. Bandgap (in eV) of 30 solids (the space group number is indicated in parenthesis) calculated non-self-consistently with MGGA functionals using Eq. (2). The GGA potential used to generate the orbitals is EV93PW91 for MVS, mRPBE for HLE17, and RPBE for all other MGGA functionals. The value in parenthesis is the difference with respect to the self-consistent VASP calculation ( $E_g^{\text{WIEN2k}} - E_g^{\text{VASP}}$ ). The second set of value in parenthesis for PBE and rSCAN is the difference with respect to CASTEP results.

Solid	PBE	TPSS	revTPSS	MVS	SCAN	rSCAN	TM	HLE17
Al <sub>2</sub> O <sub>3</sub> (167)	6.20 (0.01,0.00)	6.39 (0.08)	6.34 (0.08)	7.30 (-0.13)	7.20 (0.17)	7.12 (0.06,0.07)	6.36 (0.04)	7.17 (0.22)
AlAs (216)	1.47 (0.04,0.01)	1.59 (0.10)	1.51 (0.08)	2.33 (0.17)	1.85 (0.12)	1.87 (0.10,0.07)	1.44 (0.00)	2.76 (0.27)
AlN (186)	4.14 (-0.00,0.01)	4.21 (0.07)	4.13 (0.05)	4.89 (-0.22)	4.78 (-0.01)	4.82 (0.03,0.05)	4.16 (0.00)	4.91 (0.17)
AlP (216)	1.59 (0.01,-0.02)	1.74 (0.10)	1.64 (0.08)	2.22 (0.11)	1.96 (0.06)	1.95 (0.05,0.03)	1.60 (0.02)	2.84 (0.05)
AlSb (216)	1.22 (0.01,-0.00)	1.31 (0.04)	1.23 (0.04)	1.85 (0.05)	1.46 (0.09)	1.46 (0.01,0.00)	1.12 (-0.04)	2.05 (0.25)
Ar (225)	8.71 (-0.01,0.01)	9.35 (0.04)	9.26 (-0.01)	10.37 (-0.09)	9.58 (0.08)	9.54 (0.01,-0.02)	8.74 (0.07)	10.91 (0.07)
BeO (186)	7.37 (0.02,0.01)	7.43 (0.10)	7.37 (0.10)	8.22 (-0.21)	8.31 (0.15)	8.25 (0.06,0.07)	7.39 (0.05)	8.59 (0.12)
BN (216)	4.46 (0.01,-0.02)	4.66 (0.23)	4.47 (0.18)	5.08 (0.05)	5.06 (0.13)	5.08 (0.09,0.08)	4.48 (0.09)	5.97 (0.28)
BP (216)	1.25 (-0.02,-0.01)	1.32 (0.01)	1.19 (0.00)	1.36 (-0.09)	1.56 (-0.02)	1.44 (-0.04,0.01)	1.20 (-0.04)	2.18 (-0.05)
C (227)	4.14 (-0.01,-0.00)	4.26 (0.07)	4.10 (0.04)	4.04 (-0.15)	4.54 (-0.04)	4.38 (-0.00,0.03)	4.10 (0.01)	5.14 (0.14)
CaF <sub>2</sub> (225)	7.28 (0.00,0.02)	7.75 (0.02)	7.49 (-0.03)	8.57 (0.25)	8.04 (0.21)	8.09 (0.22,0.22)	6.90 (0.07)	9.44 (0.11)
CaO (225)	3.67 (0.04,-0.00)	3.81 (0.06)	3.72 (0.02)	4.38 (0.01)	4.45 (0.29)	4.42 (0.26,0.23)	3.61 (0.00)	4.57 (0.06)
CdSe (216)	0.71 (-0.04,-0.01)	0.94 (0.04)	0.93 (0.04)	2.24 (0.17)	1.10 (0.03)	1.18 (0.02,0.00)	0.93 (0.03)	1.71 (-0.02)
GaAs (216)	0.52 (-0.05,0.00)	0.72 (0.04)	0.76 (0.05)	2.31 (0.15)	0.80 (0.00)	0.96 (-0.04,-0.03)	0.86 (0.02)	0.79 (0.13)
GaP (216)	1.59 (-0.05,-0.01)	1.70 (0.02)	1.59 (0.02)	2.15 (0.00)	1.81 (-0.07)	1.84 (-0.06,-0.00)	1.55 (0.00)	2.25 (0.05)
Ge (227)	0.06 (-0.05,0.00)	0.20 (0.03)	0.27 (0.05)	1.76 (0.54)	0.24 (0.10)	0.39 (-0.06,-0.05)	0.42 (0.11)	0.00 (0.00)
InP (216)	0.68 (-0.03,-0.00)	0.87 (0.05)	0.85 (0.06)	1.98 (0.07)	0.98 (-0.07)	1.07 (-0.04,-0.02)	0.90 (0.04)	1.16 (0.03)
KCl (225)	5.21 (-0.00,0.01)	5.70 (-0.02)	5.59 (-0.02)	6.61 (0.14)	5.74 (-0.04)	5.77 (0.00,0.00)	5.12 (0.02)	6.88 (-0.04)
Kr (225)	7.26 (-0.01,-0.00)	7.86 (-0.03)	7.84 (-0.03)	9.22 (0.24)	8.00 (-0.04)	8.04 (0.02,0.04)	7.39 (0.04)	9.29 (-0.02)
LiCl (225)	6.33 (0.00,0.00)	6.54 (-0.01)	6.56 (-0.03)	7.75 (0.01)	7.18 (0.00)	7.12 (-0.02,-0.03)	6.52 (-0.03)	7.76 (-0.01)
LiF (225)	9.08 (0.00,0.01)	9.23 (-0.03)	9.07 (-0.11)	10.79 (0.31)	10.14 (0.16)	10.11 (0.14,0.11)	8.89 (-0.07)	10.81 (-0.01)
LiH (225)	3.08 (0.08,0.01)	3.37 (0.01)	3.64 (0.02)	3.83 (-0.19)	3.58 (-0.06)	3.54 (-0.03,-0.08)	3.16 (-0.06)	4.66 (0.04)
MgO (225)	4.71 (0.00,0.01)	4.80 (-0.00)	4.73 (-0.02)	5.88 (-0.06)	5.69 (0.16)	5.63 (0.07,0.08)	4.78 (-0.01)	5.66 (0.05)
NaCl (225)	5.11 (0.01,0.00)	5.47 (0.02)	5.41 (0.00)	6.55 (-0.01)	5.76 (-0.09)	5.76 (-0.07,-0.06)	5.13 (-0.05)	6.73 (0.02)
NaF (225)	6.33 (0.02,0.02)	6.74 (0.06)	6.50 (-0.02)	7.81 (0.11)	7.19 (0.17)	7.15 (0.07,0.08)	5.95 (-0.12)	8.38 (0.09)
Ne (225)	11.58 (-0.00,-0.01)	12.28 (0.13)	12.20 (-0.01)	13.88 (0.43)	12.97 (0.20)	13.07 (0.17,0.07)	11.52 (-0.07)	14.47 (0.21)
Si (227)	0.58 (-0.04,0.00)	0.69 (-0.01)	0.58 (-0.02)	0.87 (-0.07)	0.85 (-0.02)	0.77 (-0.05,0.01)	0.56 (-0.05)	1.57 (-0.06)
SiC (216)	1.36 (0.01,-0.03)	1.47 (0.15)	1.30 (0.10)	1.82 (-0.03)	1.78 (0.07)	1.82 (0.08,0.07)	1.33 (0.04)	2.47 (0.18)
ZnO (186)	0.82 (0.02,0.03)	0.79 (0.06)	0.61 (0.01)	1.57 (0.15)	1.32 (0.18)	1.40 (0.17,0.19)	0.55 (-0.08)	2.26 (-0.12)
ZnS (216)	2.12 (-0.03,-0.01)	2.33 (0.04)	2.26 (0.04)	3.42 (0.12)	2.60 (-0.03)	2.66 (0.00,0.00)	2.22 (-0.01)	3.23 (-0.06)

The average over all solids of the absolute difference  $|E_g^{\text{WIEN2k}} - E_g^{\text{VASP}}|$  is shown in Table II for all combinations ( $E_{xc}, \nu_{xc}$ ), i.e., all sets of orbitals (generated by the various  $\nu_{xc}$ ) plugged into all MGGA energy functionals  $E_{xc}$ . The values with the optimal orbitals (highlighted in bold) represent the statistics of the results in Table I. For all functionals except MVS the average error is below 0.1 eV. A larger value of 0.14 eV is obtained for the MVS functional with the EV93PW91 orbitals. We checked that combining the EV93 exchange potential<sup>48</sup> with other correlation potentials like LDA,<sup>51</sup> PBE,<sup>6</sup> or LYP<sup>8</sup> does not improve the MVS results.

In general, a clear correlation between the total MGGA energy and the difference in the bandgap can be observed; if a set of orbitals leads to (one of) the most negative total energy for a particular MGGA functional (quantified by the average of the total energy per cell and per electron, see Table II), then the agreement with VASP for the bandgap will be one of the best. However, choosing a set of orbitals that is not the one that minimizes the MGGA functional may seriously degrade the agreement with VASP. For instance, the mRPBE orbitals, which are the optimal for the MGGA HLE17, lead to

rather inaccurate results for all other MGGAs (the disagreement with VASP is 0.8-0.9 eV). Among all sets of orbitals that we have considered, the Sloc orbitals lead most of the time to the least negative MGGA total energy and, consequently, to the worst agreement with VASP results for the bandgap except with HLE17. We just note that in the case of the (r)SCAN functional, the EV93PW91 orbitals, despite being less optimal than the RPBE ones for the total energy, lead to slightly better agreement between WIEN2k and VASP for the bandgap. However, the differences are at the level of 0.01-0.02 eV, which is very small and of the same order as errors that could come from other parameters like the basis set size or the pseudopotential. A graphical illustration of the detailed results is shown in Fig. 1 for the revTPSS functional when it is evaluated using the orbitals obtained from some of the best potentials. From Fig. 1(a), which compares the revTPSS total energies, we can see that the ordering of the potentials, except HCTH407, is the same for all solids. The results with the HCTH407 orbitals alternate with those from the other sets of orbitals. The results for the bandgap in Fig. 1(b) show that using the RPBE orbitals (the optimal ones for the revTPSS total energy) does not systematically lead to the smallest difference

TABLE II. Average (in eV) of the absolute difference between the non-self-consistent (WIEN2K) and self-consistent (VASP) bandgaps. The non-self-consistent bandgaps were calculated with Eq. (2) for various MGGA functionals (corresponding to the columns) by using orbitals that were generated by various potentials (corresponding to the rows). The number in parenthesis is the average of  $(E_{\text{tot}}^{\text{uc}} - E_{\text{tot}}^{\text{uc},0})/N_{\text{el}}^{\text{uc}}$  where  $E_{\text{tot}}^{\text{uc},0}$  (in mRy) is the lowest total MGGA energy among all those calculated using the different sets of orbitals and  $N_{\text{el}}^{\text{uc}}$  is the number of electrons per unit cell. The results for the combination  $(E_{\text{xc}}, v_{\text{xc}})$  that was used for the bandgaps in Table I are in bold.

	TPSS	revTPSS	MVS	SCAN	rSCAN	TM	HLE17
RPBE	<b>0.06 (0.0)</b>	<b>0.04 (0.0)</b>	0.15 (0.2)	<b>0.10 (0.0)</b>	<b>0.07 (0.0)</b>	<b>0.04 (0.0)</b>	0.90 (4.9)
PBE	0.06 (0.0)	0.05 (0.0)	0.16 (0.5)	0.11 (0.1)	0.08 (0.1)	0.04 (0.0)	0.92 (5.3)
PBEsol	0.13 (0.2)	0.11 (0.2)	0.27 (0.7)	0.17 (0.3)	0.17 (0.3)	0.11 (0.2)	0.98 (6.3)
HCTH407	0.14 (0.3)	0.15 (0.3)	0.16 (0.3)	0.13 (0.1)	0.12 (0.1)	0.18 (0.4)	0.74 (4.0)
EV93PW91	0.10 (0.5)	0.10 (0.4)	<b>0.14 (0.0)</b>	0.08 (0.3)	0.06 (0.3)	0.09 (0.3)	0.87 (4.6)
LDA	0.13 (0.7)	0.10 (0.8)	0.18 (1.7)	0.18 (0.9)	0.15 (0.9)	0.10 (0.8)	0.97 (7.7)
AK13	0.40 (2.6)	0.44 (2.6)	0.63 (1.7)	0.49 (2.4)	0.48 (2.3)	0.53 (2.8)	0.91 (4.2)
LB94	0.41 (3.7)	0.44 (4.1)	0.58 (5.3)	0.41 (3.8)	0.44 (3.8)	0.48 (4.4)	0.55 (4.5)
mRPBE	0.81 (4.9)	0.83 (5.3)	0.88 (4.8)	0.80 (4.6)	0.83 (4.6)	0.89 (5.3)	<b>0.10 (0.0)</b>
HLE16	0.91 (6.3)	0.92 (6.7)	0.91 (5.8)	0.89 (5.9)	0.90 (5.8)	0.99 (6.8)	0.21 (0.5)
Sloc	1.60 (12.0)	1.61 (12.6)	1.58 (12.4)	1.55 (11.6)	1.56 (11.6)	1.67 (12.9)	0.78 (2.8)

$E_{\text{g}}^{\text{WIEN2K}} - E_{\text{g}}^{\text{VASP}}$ , however on average the difference is the smallest (0.04 eV, see Table II). The results for the revTPSS bandgap with the PBEsol and HCTH407 orbitals [not shown in Fig. 1(b)] exhibit for a few cases (e.g., Ge with PBEsol) rather large errors.

We mention that Lima *et al.*<sup>62</sup> proposed to approximate the potential  $v_{\text{xc}}^{\text{B}}$  of a functional  $E_{\text{xc}}^{\text{B}} = \int \epsilon_{\text{xc}}^{\text{B}} d^3r$  as the rescaling of the potential of another functional A:  $v_{\text{xc}}^{\text{B}} \approx (\epsilon_{\text{xc}}^{\text{B}}/\epsilon_{\text{xc}}^{\text{A}}) v_{\text{xc}}^{\text{A}}$ . This method may be useful when the potential  $v_{\text{xc}}^{\text{B}}$  is not implemented, as in our case here with MGGAs. We tested this scheme for a few cases, including A = PBE, RPBE, or EV93PW91 and B = SCAN or MVS, to obtain an approximate (and multiplicative) MGGA potential that is used to calculate the orbitals that are then plugged into the corresponding total-energy MGGA functional. However, the results (not shown) are typically worse than those obtained with several of the GGA potentials, meaning that the orbitals obtained with  $v_{\text{xc}}^{\text{B=MGGA}}$  are not particularly close to the true MGGA orbitals. Thus the method does not seem to be really useful for our purpose.

In summary, we have shown that the use of total energies [Eq. (2)] to calculate the bandgap of MGGA functionals can lead to very accurate results even when GGA orbitals are used. However, it is important to choose reasonable orbitals, i.e., orbitals that satisfy the variational principle as much as possible. Luckily, once a GGA potential to generate the orbitals has been shown to be appropriate for a MGGA functional in a few cases, then it appears to be rather safe to use it for other solids. Thus, this scheme allows to obtain the bandgap with MGGA functionals when the corresponding potential is not implemented. In principle, this simple procedure can be applied to any kind of (new) energy functionals, whose self-consistent implementation would require intense effort.

J.D. and P.B. acknowledge support from the Austrian Science Fund (FWF) through project W1243 (Solids4Fun). S.B. acknowledges partial support from the DFG through the project BO 4280/8-1. Computational resources were provided by the Leibniz Supercomputing Centre through the projects

pr62ja. M.A.L.M. acknowledges partial support from the German DFG through the project MA6787/6-1. A.P.B. acknowledges support from the Collaborative Computational Project for NMR Crystallography (CCP-NC) and UKCP Consortium, both funded by the Engineering and Physical Sciences Research Council (EPSRC) under Grants No. EP/M022501/1 and No. EP/P022561/1, respectively. Some of the calculations were run using the STFC Scientific Computing Department's SCARF cluster.

- <sup>1</sup>P. Hohenberg and W. Kohn, Phys. Rev. **136**, B864 (1964).
- <sup>2</sup>W. Kohn and L. J. Sham, Phys. Rev. **140**, A1133 (1965).
- <sup>3</sup>A. Seidl, A. Görling, P. Vogl, J. A. Majewski, and M. Levy, Phys. Rev. B **53**, 3764 (1996).
- <sup>4</sup>J. P. Perdew, R. G. Parr, M. Levy, and J. L. Balduz, Jr., Phys. Rev. Lett. **49**, 1691 (1982).
- <sup>5</sup>L. J. Sham and M. Schlüter, Phys. Rev. Lett. **51**, 1888 (1983).
- <sup>6</sup>J. P. Perdew, K. Burke, and M. Ernzerhof, Phys. Rev. Lett. **77**, 3865 (1996), **78**, 1396(E) (1997).
- <sup>7</sup>A. D. Becke, Phys. Rev. A **38**, 3098 (1988).
- <sup>8</sup>C. Lee, W. Yang, and R. G. Parr, Phys. Rev. B **37**, 785 (1988).
- <sup>9</sup>J. Heyd, J. E. Peralta, G. E. Scuseria, and R. L. Martin, J. Chem. Phys. **123**, 174101 (2005).
- <sup>10</sup>E. Kraisler and L. Kronik, J. Chem. Phys. **140**, 18A540 (2014).
- <sup>11</sup>A. Görling, Phys. Rev. B **91**, 245120 (2015).
- <sup>12</sup>J. P. Perdew and A. Zunger, Phys. Rev. B **23**, 5048 (1981).
- <sup>13</sup>P. Mori-Sánchez, A. J. Cohen, and W. Yang, Phys. Rev. Lett. **100**, 146401 (2008).
- <sup>14</sup>J. P. Perdew, Adv. Quantum Chem. **21**, 113 (1990).
- <sup>15</sup>F. Tran and P. Blaha, Phys. Rev. Lett. **102**, 226401 (2009).
- <sup>16</sup>R. Armiento and S. Kümmel, Phys. Rev. Lett. **111**, 036402 (2013).
- <sup>17</sup>P. Verma and D. G. Truhlar, J. Phys. Chem. Lett. **8**, 380 (2017).
- <sup>18</sup>F. Della Sala, E. Fabiano, and L. A. Constantin, Int. J. Quantum Chem. **116**, 1641 (2016).
- <sup>19</sup>A. D. Becke, J. Chem. Phys. **98**, 5648 (1993).
- <sup>20</sup>S. Kümmel and L. Kronik, Rev. Mod. Phys. **80**, 3 (2008).
- <sup>21</sup>W. Yang, A. J. Cohen, and P. Mori-Sánchez, J. Chem. Phys. **136**, 204111 (2012).
- <sup>22</sup>Z.-h. Yang, H. Peng, J. Sun, and J. P. Perdew, Phys. Rev. B **93**, 205205 (2016).
- <sup>23</sup>J. P. Perdew, W. Yang, K. Burke, Z. Yang, E. K. U. Gross, M. Scheffler, G. E. Scuseria, T. M. Henderson, I. Y. Zhang, A. Ruzsinszky, H. Peng, J. Sun, E. Trushin, and A. Görling, Proc. Natl. Acad. Sci. U.S.A. **114**, 2801 (2017).

- <sup>24</sup>J. Sun, A. Ruzsinszky, and J. P. Perdew, Phys. Rev. Lett. **115**, 036402 (2015).
- <sup>25</sup>E. B. Isaacs and C. Wolverton, Phys. Rev. Materials **2**, 063801 (2018).
- <sup>26</sup>Y. Zhang, D. A. Kitchaev, J. Yang, T. Chen, S. T. Dacek, R. A. Sarmiento-Pérez, M. A. L. Marques, H. Peng, G. Ceder, J. P. Perdew, and J. Sun, npj Comput. Mater. **4**, 9 (2018).
- <sup>27</sup>C. Lane, J. W. Furness, I. G. Buda, Y. Zhang, R. S. Markiewicz, B. Barbiellini, J. Sun, and A. Bansil, Phys. Rev. B **98**, 125140 (2018).
- <sup>28</sup>J. Varignon, M. Bibes, and A. Zunger, Phys. Rev. B **100**, 035119 (2019).
- <sup>29</sup>S. Jana, A. Patra, and P. Samal, J. Chem. Phys. **149**, 044120 (2018).
- <sup>30</sup>Y. Fu and D. J. Singh, Phys. Rev. Lett. **121**, 207201 (2018).
- <sup>31</sup>D. Mejía-Rodríguez and S. B. Trickey, Phys. Rev. B **100**, 041113(R) (2019).
- <sup>32</sup>R. Neumann, R. H. Nobes, and N. C. Handy, Mol. Phys. **87**, 1 (1996).
- <sup>33</sup>A. V. Bienvenu and G. Knizia, J. Chem. Theory Comput. **14**, 1297 (2018).
- <sup>34</sup>D. Mejia-Rodriguez and S. B. Trickey, Phys. Rev. B **98**, 115161 (2018).
- <sup>35</sup>Á. Morales-García, R. Valero, and F. Illas, J. Phys. Chem. C **121**, 18862 (2017).
- <sup>36</sup>W. Chen, G. Miceli, G.-M. Rignanese, and A. Pasquarello, Phys. Rev. Materials **2**, 073803 (2018).
- <sup>37</sup>E. Trushin, M. Betzinger, S. Blügel, and A. Görling, Phys. Rev. B **94**, 075123 (2016).
- <sup>38</sup>V. Vlček, H. R. Eisenberg, G. Steinle-Neumann, L. Kronik, and R. Baer, J. Chem. Phys. **142**, 034107 (2015).
- <sup>39</sup>M. R. Pederson, A. Ruzsinszky, and J. P. Perdew, J. Chem. Phys. **140**, 121103 (2014).
- <sup>40</sup>J. Tao, J. P. Perdew, V. N. Staroverov, and G. E. Scuseria, Phys. Rev. Lett. **91**, 146401 (2003).
- <sup>41</sup>J. P. Perdew, A. Ruzsinszky, G. I. Csonka, L. A. Constantin, and J. Sun, Phys. Rev. Lett. **103**, 026403 (2009), **106**, 179902 (2011).
- <sup>42</sup>J. Sun, J. P. Perdew, and A. Ruzsinszky, Proc. Natl. Acad. Sci. U.S.A. **112**, 685 (2015).
- <sup>43</sup>A. P. Bartók and J. R. Yates, J. Chem. Phys. **150**, 161101 (2019).
- <sup>44</sup>J. Tao and Y. Mo, Phys. Rev. Lett. **117**, 073001 (2016).
- <sup>45</sup>P. Verma and D. G. Truhlar, J. Phys. Chem. C **121**, 7144 (2017).
- <sup>46</sup>B. Hammer, L. B. Hansen, and J. K. Nørskov, Phys. Rev. B **59**, 7413 (1999).
- <sup>47</sup>J. P. Perdew, A. Ruzsinszky, G. I. Csonka, O. A. Vydrov, G. E. Scuseria, L. A. Constantin, X. Zhou, and K. Burke, Phys. Rev. Lett. **100**, 136406 (2008), **102**, 039902(E) (2009).
- <sup>48</sup>E. Engel and S. H. Vosko, Phys. Rev. B **47**, 13164 (1993).
- <sup>49</sup>J. P. Perdew, J. A. Chevary, S. H. Vosko, K. A. Jackson, M. R. Pederson, D. J. Singh, and C. Fiolhais, Phys. Rev. B **46**, 6671 (1992), **48**, 4978(E) (1993).
- <sup>50</sup>A. D. Boese and N. C. Handy, J. Chem. Phys. **114**, 5497 (2001).
- <sup>51</sup>J. P. Perdew and Y. Wang, Phys. Rev. B **45**, 13244 (1992), **98**, 079904(E) (2018).
- <sup>52</sup>R. van Leeuwen and E. J. Baerends, Phys. Rev. A **49**, 2421 (1994).
- <sup>53</sup>K. Finzel and A. I. Baranov, Int. J. Quantum Chem. **117**, 40 (2017).
- <sup>54</sup>P. Blaha, K. Schwarz, G. K. H. Madsen, D. Kvasnicka, J. Luitz, R. Laskowski, F. Tran, and L. D. Marks, *WIEN2k: An Augmented Plane Wave plus Local Orbitals Program for Calculating Crystal Properties* (Vienna University of Technology, Austria, 2018).
- <sup>55</sup>D. J. Singh and L. Nordström, *Planewaves, Pseudopotentials, and the LAPW Method, 2nd ed.* (Springer, New York, 2006).
- <sup>56</sup>F. Karsai, F. Tran, and P. Blaha, Comput. Phys. Commun. **220**, 230 (2017).
- <sup>57</sup>P. Borlido, T. Aull, A. W. Huran, F. Tran, M. A. L. Marques, and S. Botti, J. Chem. Theory Comput. **15**, 5069 (2019).
- <sup>58</sup>G. Kresse and J. Furthmüller, Phys. Rev. B **54**, 11169 (1996).
- <sup>59</sup>P. E. Blöchl, Phys. Rev. B **50**, 17953 (1994).
- <sup>60</sup>M. C. Payne, M. P. Teter, D. C. Allan, T. A. Arias, and J. D. Joannopoulos, Rev. Mod. Phys. **64**, 1045 (1992).
- <sup>61</sup>S. J. Clark, M. D. Segall, C. J. Pickard, P. J. Hasnip, M. I. J. Probert, K. Refson, and M. C. Payne, Z. Kristallogr.-Cryst. Mater. **220**, 567 (2005).
- <sup>62</sup>M. P. Lima, L. S. Pedroza, A. J. R. da Silva, A. Fazzio, D. Vieira, H. J. P. Freire, and K. Capelle, J. Chem. Phys. **126**, 144107 (2007).